Investigation of the Electronic Spectra and Excited-State Geometries of Poly(*para*-phenylene vinylene) (PPV) and Poly(*para*-phenylene) (PP) by the Symmetry-Adapted Cluster Configuration Interaction (SAC-CI) Method

Biswajit Saha, Masahiro Ehara, and Hiroshi Nakatsuji*

Department of Synthetic Chemistry and Biological Chemistry, Graduate School of Engineering, Kyoto University, Katsura, Nishikyo-ku, Kyoto 615-8510, Japan

Received: December 8, 2006; In Final Form: April 23, 2007

The symmetry-adapted cluster-configuration interaction (SAC-CI) method has been used to investigate the optical and geometric properties of the oligomers of poly(*para*-phenylene vinylene) (PPV) and poly(*para*-phenylene) (PP). Vertical singlet and triplet absorption spectra and emission spectra have been calculated accurately; the mean average deviation from available experimental results lies within 0.2 eV. The chain length dependence of the transition energies has been improved in comparison to earlier TDDFT and MRSDCI calculations. The present analysis suggests that conventional TDDFT with the B3LYP functional should be used carefully, as it can provide inaccurate estimates of the chain length dependence of the excitation energies of these molecules with long π conjugation. The T_1 state was predicted to be at a lower energy, by 1.0−1.5 eV for PPV and by 0.9−1.7 eV for PP, than the S_1 state, which indicates a localized T_1 state with large exchange energy. By calculating the SAC-CI electron density difference between the ground and excited states, the geometry relaxations due to excitations can be analyzed in detail using electrostatic force theory. For *trans*-stilbene, the doubly excited 2^1A_g state was studied, and the calculated transition energy of 4.99 eV agrees very well with the experimental value of 4.84 eV. In contrast to previous ab initio calculations, we predict this doubly excited 2^1A_g state to lie above the 1^1B_u state.

Introduction

Research on poly(*para*-phenylene vinylene) (PPV) and poly(*para*-phenylene) (PP) continues unabated because of their potential applications as active organic light-emitting diodes in electro-optic devices.[1−3] Many experimental studies have been performed on their spectral properties, as well as on the effects of structural and chemical substitution.[4−12] To understand the experimental results and to predict the photophysical and optical properties of these conjugated molecules, various quantum chemical calculations have also been performed. Electronic excitations in these oligomers have been investigated by means of semiempirical methods,[13−18] density matrix renormalization group (DMRG) theory,[19] time-dependent density functional theory (TDDFT),[20,21] and also the multireference singles−doubles CI (MRSDCI) method.[22,23] In most of these theoretical studies, mainly the lowest singlet excitation was reported, although triplet states are believed to be the dominant species formed upon charge recombination that yields electroluminescence. This is because, according to simple spin statistics, three-quarters of the excitons formed are triplets.[1,24] Thus, to produce better materials and to gain deeper insight into these polymers, knowledge of their triplet states is also useful.

S_0-S_1 transition energies of PPV with *n* phenylene vinylene units (PPV*n*) calculated by TDDFT with the B3LYP functional[20] showed that, for PPV3 and PPV4, the computed values deviate significantly from the experimental transition energies, being 0.36 and 0.66 eV, respectively. In addition, larger deviations from the experimental transition energies were obtained in TDDFT computations as the oligomer chain length increased.[20,21] The transition energies of PPV*n* estimated by MRSDCI calculations also deviated from the available experimental values, and the chain length dependence of the triplet states could not be reproduced properly.[22] Theoretical investigations of the fluorescence spectra of PPV*n* have been limited to AM1-CAS-CI,[25] restricted CI singles (RCIS),[12] and TDDFT-(B3LYP)[21] calculations. Thus, a reliable theoretical method for predicting optical properties of these OLED molecules has not yet been established.

An ab initio Hartree−Fock study on the electronic structure of various conjugated polymers including poly(*para*-phenylene) was performed by Brédas et al.[26,27] Soos et al. used the Pariser−Parr−Pople (PPP) model to investigate the lowest singlet state of different conjugated phenylene polymers.[28] The geometric and optical properties of poly(*para*-phenylene) have been investigated using the semiempirical AM1 method.[17] The results obtained from TDDFT[20] calculations agreed well with the experimental results, although, for longer PP*n* molecules, larger deviations were found, and also the slope of the dependence of the excitation energy on the inverse of the chain length differed from that observed in experiment. They concluded that the TDDFT calculations were the source of this inconsistency. A detailed experimental and semiempirical investigation on the triplet exchange energy of polymers such as poly(*para*-phenylene) and poly(*para*-phenylene vinylene) was reported by Köhler et al.[29]

Furthermore, in most of the earlier ab initio calculations, electron correlations were not included properly; as a result, the correlated doubly excited $2A_g$ states could not be estimated correctly. Therefore, it is a challenging task to calculate the

* To whom correspondence should be addressed. E-mail: hiroshi@sbchem.kyoto-u.ac.jp.

10.1021/jp068441d CCC: $37.00
Published on Web 06/02/2007

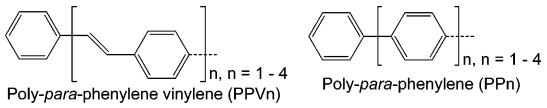

Figure 1. Poly(*para*-phenylene vinylene) (PPV*n*) and poly(*para*-phenylene) (PP*n*) studied by the SAC-CI method. *n* corresponds to the number of repeat units.

singlet and triplet excited states consistently and accurately, to such extensive conjugation lengths, using a high-level theory, such as the symmetry-adapted cluster-configuration interaction (SAC-CI) method, and also to estimate the so-called doubly excited $2A_g$ state of PPV*n*.

The structures of the PPV*n* in the ground state were estimated by semiempirical methods,[30,31] complete active space self-consistent field (CASSCF),[32] DFT[33] for $n = 1$ and by Austin Model 1 (AM1)[13] for $n = 1-4$. The geometries for the S_1 and T_1 excited states of PPV*n* for $n = 1-3$ calculated by AM1 and using bond-order/bond-length (BOBL) relationships on the basis of the INDO/MRD-CI bond orders[13,34] are also available. First-principles local-density band structure calculations were performed on ground-state structure of the crystalline poly(*para*-phenylene) by Ambrosch-Draxl et al.[35] while Zojer et al.[17] presented a semiempirical AM1 calculations on the ground-state geometry of neutral and charged poly(*para*-phenylene). Ground-state structural properties of poly(*para*-phenylene vinylene) and poly(*para*-phenylene) were also investigated by density-functional and plane-wave approach.[36,37] Optimized ground-state and S_1 and T_1 excited-state geometries of PP*n* were calculated by Pogantsch et al.[20] using DFT/TDDFT method. Recently, Alves-Santos et al. applied DFT method to study the structural properties of poly(*para*-phenylene).[38]

Widely employed semiempirical and TDDFT methods have been used successfully to obtain a qualitative understanding of many properties, particularly absorption spectra and nonlinear optical spectra. To improve this theoretical understanding, calculations that include the electron correlation effect are necessary. The SAC-CI method[39−41] has been shown to provide accurate descriptions of electron correlations for many-body systems and can be efficiently applied to a wide range of problems within the same framework. This method is size-consistent and size-intensive, and therefore, it is suitable for investigating molecular systems with repeated units such as oligomers and polymers with long π-conjugated chains. Recently, the method has been developed and extended for calculations on very large molecular systems and molecular crystals because of this advantage.[42] In the present investigation, we performed a systematic study of the absorption spectra and fluorescence spectra of PPV*n* with $n = 1-4$ phenylene vinylene units and PP*n* with $n = 1-4$ phenylene units, by the SAC-CI method. We report herein the lowest singlet (S_0-S_1) and triplet (S_0-T_1) transitions and the fluorescence spectra (S_1-S_0) of these oligomers. The present results are compared with the available experimental and theoretical values. Ground- (S_0) and lowest-excited-state (S_1 and T_1) geometries for PPV1, PPV2, PPV3, PP1, and PP2 are also estimated by the SAC/SAC-CI method for which an analytical form of the energy gradient is available. Moreover, the geometry changes due to excitations are discussed in detail in light of the electrostatic force (ESF) theory proposed by Nakatsuji.[43,44]

Computational Details

The excitation energies and excited-state geometries for the lowest singlet and triplet excited states of PPV*n* and PP*n* consisting of $n = 1-4$ repeat units, as shown in Figure 1, were calculated. The ground-state geometries were optimized using the B3LYP/6-31G(d) and SAC/6-31G(d) methods with the constraints of planar C_{2h} symmetry for PPV*n* and nonplanar D_2 symmetry for PP*n*. For the ground states of PPV1 and PPV2, the SAC method predicted that the planar geometry is stable. Because the SAC/SAC-CI geometry optimization is expensive for higher oligomers, we used DFT-optimized ground-state geometries for calculating the absorption spectra to make consistent comparisons. A comparison of SAC- and DFT-optimized ground-state geometries and corresponding vertical excitation energies is provided in the Supporting Information. We found that the geometries optimized by SAC did not differ much from the DFT geometries and that the differences did not have much of an effect on the vertical excitation energies. For calculating the vertical excitations and fluorescence emissions by the SAC-CI SD-*R* method, the double-ζ basis set due to Huzinaga and Dunning[45] plus one polarization function [4s2p1d/2s] was employed. The CIS and SAC-CI SD-R geometry optimizations, with the constraints of planar C_{2h} symmetry for PPV*n* and nonplanar D_2 symmetry for PP*n*, were also performed with Huzinaga−Dunning[45] basis set plus one polarization function [4s2p1d/2s]. Fluorescence spectra of both PPV*n* and PP*n* were calculated using the CIS-optimized geometries. The results of the CIS and SAC-CI geometry optimizations are also compared in Supporting Information, and the differences in their structure parameters are small. The SAC-CI general-*R* calculation[46,47] considering up to quadruple excitations was performed only to calculate the vertical excitation energy of the doubly excited state (2^1A_g) of PPV1.

To reduce the computational effort, the perturbation selection scheme was employed.[48] LevelTwo accuracy was used to calculate the absorption and fluorescence spectra. The threshold of the linked terms for the ground state was set to $\lambda_g = 5.0 \times 10^{-6}$ au. The unlinked terms were described as the product of the linked operators with SDCI coefficients larger than 0.005. For excited states, the threshold of the linked doubles was set to $\lambda_e = 5.0 \times 10^{-7}$ au. The thresholds of the CI coefficients for calculating the unlinked operators were 0.05 and 0.00 for the *R* and *S* operators, respectively. LevelOne accuracy was used for the geometry optimizations of PPV1, PPV2, PP1, and PP2. The thresholds of the linked terms for LevelOne were set to $\lambda_g = 1.0 \times 10^{-5}$ au and $\lambda_e = 1.0 \times 10^{-6}$ au. The 1s orbitals of the first-row atoms and their counterpart molecular orbitals were kept fixed and excluded from the active space, and therefore, the active spaces used for calculations were 220 for PPV1 and 188, 280, 372, and 464 for PP*n* with $n = 1-4$, respectively. For larger PPV oligomers, the 1s orbitals of the first-row atoms and the virtual orbitals above 1.5 au were kept fixed and excluded from the active space, and therefore, the active spaces used in the present calculation were 221, 290, and 397 for PPV*n* with $n = 2-4$, respectively. The Gaussian 03 suite of programs[49] was utilized for all of these computations. Interested reader can obtain much information on the SAC-CI method from the articles by Nakatsuji and coauthors.[39−42,46]

Absorption and Emission Spectra

Poly(*para-phenylene vinylene) (PPVn, n = 1, ..., 4).* The vertical excitation energies from the ground state (S_0) to singlet excited state (S_1) and triplet excited state (T_1) were calculated by the SAC-CI method using the B3LYP/6-31G(d)-optimized ground-state geometry. The ground-state structure of PPV*n* is considered to have planar C_{2h} symmetry. A comparison of the lowest singlet vertical excitation energy for PPV*n* to the experimental result[12] and other computed values[19−22,25] is shown

TABLE 1: Vertical Excitation Energies (ΔE) and Oscillator Strengths (f) for the Lowest Singlet (1^1B_u) Excited States of PPVn with $n = 1-4$

	expt[a] (ΔE, eV)		SAC-CI		TDDFT		ΔE (eV)		
PPVn	dioxane[b]	vacuum[c]	ΔE (eV)	f	ΔE (eV)	f	AM1-CAS-CI[g]	DMRG[h]	MRSDCI[i]
PPV1	4.03	4.19	4.21	0.977	4.35,[d] 4.03[e]	0.682,[d] 0.99[e]	4.08	4.17	4.48, 4.34
PPV2	3.47	3.69	3.57	1.762	3.35,[d] 3.23[e]	1.576,[d] 1.84[e]	3.61	3.52	4.11, 3.91
PPV3	3.22	3.47	3.18	2.402	2.90,[d] 2.84[e]	2.365,[d] 2.59[e]	3.34	3.18	3.93, 3.65
PPV4	3.10	3.35	3.09	2.916	2.64,[d] 2.62[e]	3.093,[d] 3.28[e]	3.18	2.99	3.83, 3.46

[a] From ref 12. [b] Extracted from Figure 2 of ref 12. [c] From ref 12; Table 1 corrected with equilibrium energy. [d] From ref 21. [e] From ref 20. [g] From ref 25. [h] From ref 19. [i] From ref 22.

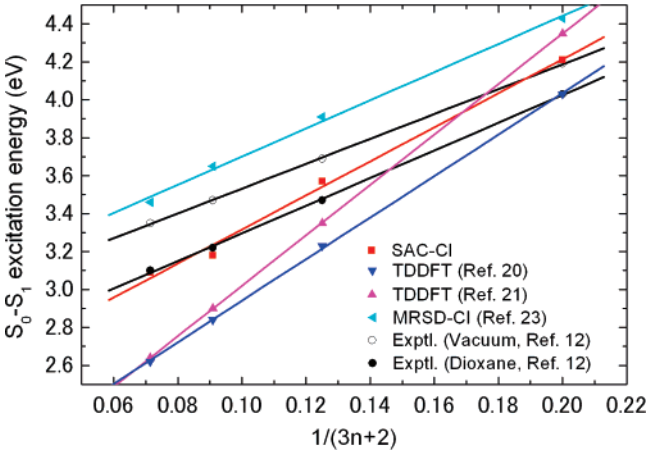

Figure 2. Comparison of SAC-CI S_0-S_1 transition energies of PPVn with experimental and other computational results.

in Table 1. The present transition energies agree very well with the available experimental values; the mean average deviation lies within 0.2 eV, and the maximum deviation is 0.29 eV. The lowest singlet $\pi-\pi^*$ transition 1^1B_u is a dipole-allowed transition with a large oscillator strength, and the calculated transition energy decreases as the conjugation length increases, i.e., the transition becomes red-shifted with increasing chain length. For this transition, the oscillator strength also increases with increasing conjugation length. Our computed transition energies agree very well with those estimated by the DMRG method;[19] the mean average deviation lies within 0.05 eV, whereas the MRSDCI[22] predicted values that are consistently about 0.4 eV high. If a correction of about 0.4 eV is applied, the MRSD-CI results also agree well with the experimental values. This deviation can be ascribed to the zero-point energy and the PPP Hamiltonian.[22] A comparison of the present data with experimental and other theoretical data is shown in Figure 2. Excitation energies are plotted as a function of $1/(3n + 2)$, which represents the conjugation length. As the chain length grows, larger deviations are obtained when the present results are compared with TDDFT calculations.[20,21] It is evident from this figure that, for these oligomers, the SAC-CI method produces a better chain length dependence for the lowest singlet transition energies than the previous TDDFT calculations with the B3LYP functional. This shows that conventional TDDFT with the B3LYP functional should be used carefully for the excitation energies of molecules with long π-conjugated chains. The zero-point-energy correction to the excitation energy was estimated as -0.07 eV for PPV1; the theoretical value approaches the experimental value with this correction. For calculating the zero-point-energy correction, ground-state and lowest excited-state harmonic frequencies were calculated using the Hartree−Fock and CIS levels of theories, respectively, at the geometries optimized by the respective methods. In the experimental work,[12] the solvent effect was examined, and the spectra obtained in vacuo were extrapolated. By preliminary calculations, the solvent effect on the S_1 excitation energy of PPV1 was estimated to be -0.166 eV in dioxane according to the polarizable continuum model (PCM)[50] at the CIS level, and this effect improves the results compared to the experimental values; however, a more consistent method is expected for detailed calculations. The central vinylene C═C bond relates to the bonding and antibonding overlaps of the π orbitals in the HOMO and LUMO, respectively, whereas the opposite phase relationships are seen along the vinylene C−C bond as a result of excitation. As in most π-conjugated systems, the S_1 state mainly corresponds to a single excitation from the HOMO to the LUMO.

TABLE 2: Vertical Excitation Energies (eV) for the Lowest Triplet Excited States (1^3B_u) of PPVn with $n = 1-4$.

PPVn	SAC-CI	DMRG[a]	MRSDCI[b]
PPV1	2.65	2.65	2.66, 2.20
PPV2	2.24	2.16	2.64, 2.19
PPV3	2.02	1.95	2.63, 2.22
PPV4	1.98	1.84	2.62, 2.21

[a] From ref 19. [b] From ref 22.

The asymmetric 1^1B_u state should be below the two-photon symmetric 2^1A_g state at their equilibrium geometries, which must be satisfied so that the material becomes luminescent. We do not report this 2^1A_g state systematically in the present article, but rather performed the SAC-CI general-R calculation[46,47] considering up to quadruple excitations only for PPV1. We obtained a value of 4.99 eV for the 2^1A_g state, which is energetically above the 1^1B_u state at 4.21 eV. The experimental energy for this state is 4.84 eV.[51] Although earlier coupled-cluster singles and doubles equation-of-motion (CCSD-EOM) calculations with the PPP Hamiltonian and the DMRG method computed the 2^1A_g state at lower values of 4.18 and 4.09 eV, respectively, they estimated this state to be energetically below the 1^1B_u state.[52] Semiempirical full CI calculations using the PPP model reproduced the correct ordering of these ionic 1^1B_u and covalent 2^1A_g states.[53] From our experience, we found that, for these so-called doubly excited states, inclusion of the configurations up to quadruple excitations is necessary to reproduce the excited states in correct order and to calculate the excitation energies accurately.[54]

In addition to the singlet transition, we also report the lowest triplet ($S_0 \rightarrow T_1$) transition of PPVn and compare the results to the available data in Table 2. As for the S_1 state, the T_1 state also mainly corresponds to a single excitation from the HOMO to the LUMO. This 1^3B_u state also shows a trend similar to that of the 1^1B_u state as conjugation length increases. The singlet−triplet splitting decreases with increasing chain length. In all cases, we find that the 1^3B_u state is on the order of 1.0−1.5 eV below the 1^1B_u state, which indicates that the localized triplet state has a larger exchange energy, in agreement with experimental observations.[55] Large values for the singlet−triplet splitting were also obtained for polyacenes (1.3 eV),[56] for terthiophene (1.75 eV),[57] and for various conjugated polymers.[29] We find that the $1^1B_u-1^3B_u$ gap decreases in inverse proportion

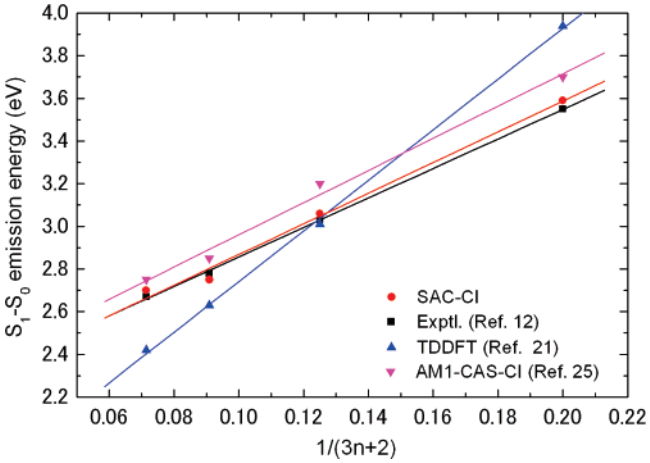

Figure 3. Evolution of S_1-S_0 emission energies as a function of the inverse conjugation length, $1/(3n + 2)$, of PPV*n*.

TABLE 3: Lowest Singlet (1^1B_u) Emission Energies (ΔE) and Oscillator Strengths (f) of PPV*n* with $n = 1-4$

	expt[a]	SAC-CI		TDDFT[b]		AM1-CAS-CI[c]
PPV*n*	ΔE (eV)	ΔE (eV)	f	ΔE (eV)	f	ΔE (eV)
PPV1	3.55	3.59	1.082	3.94	0.717	3.70
PPV2	3.03	3.06	1.757	3.01	1.715	3.20
PPV3	2.78	2.75	2.311	2.63	2.570	2.85
PPV4	2.67	2.70	2.667	2.42	3.338	2.75

[a] From ref 12. [b] From ref 21. [c] From ref 25.

to the length of the oligomers following a $1/n$ law as shown in the Supporting Information, which is also corroborated by experimental observations on PPV derivatives[55] and other theoretical results.[19] The deviation from linearity for PPV2 is ascribed to the selection of excitation operators in the SAC-CI calculations. This trend is expected, as the exchange energy decreases with increasing oligomer length. In contrast, INDO/MDR-CI[13] and MRSDCI[22] calculations showed that, whereas the $X^1A_g-1^1B_u$ gap decreased as the chain length increased, the $X^1A_g-1^3B_u$ gap remained almost constant with increasing chain length. The triplet transition energies estimated by the present computations and other theoretical methods are compared in the Supporting Information.

The SAC-CI emission spectra for PPV*n* are summarized in Table 3 and compared with available experimental[12] and other theoretical[21,25] values. The present absorption and fluorescence spectra agree very well with the available experimental spectra,[12] as shown in the Supporting Information. A comparison with other computations and experimental results on the evolution of S_1-S_0 emission energies with number of repeat unit (n) is shown in Figure 3. The experimental values were evaluated from the emission spectra reported in ref 12. Similar trends with increasing number of repeat units were obtained in the present computations and in AM1-CAS-CI caluculations,[25] although the AM1-CAS-CI-estimated energy values were consistently below the present values. However, the TDDFT[21] and INDO/SCI[7] values showed larger deviations from the experimental values than the present results.

Poly(*para*-phenylene) (PP*n*, $n = 1, ..., 4$). The vertical excitation energies from the ground state (S_0) to the singlet excited state (S_1) and the triplet excited state (T_1) were calculated by the SAC-CI method using the B3LYP/6-31G(d)-optimized ground-state geometry. The ground-state structure of PP*n* was considered to have nonplanar D_2 symmetry (the signs of the inter-ring torsion angles were assumed to be alternating). We also performed calculations for PP*n* with a planar (D_{2h} symmetry) ground-state structure.

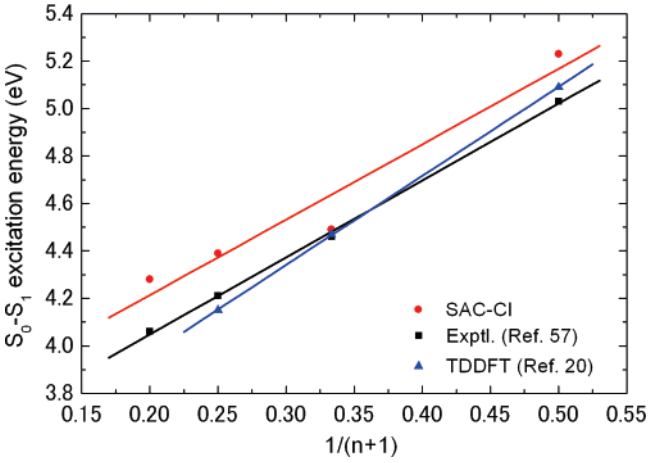

Figure 4. Comparison of SAC-CI S_0-S_1 transition energies of PP*n* with experimental and other computational results.

TABLE 4: Vertical Excitation Energies (ΔE) and Oscillator Strengths (f) for the Lowest Singlet Excited States of PP*n* with $n = 1-4$

	expt[a]	SAC-CI (nonplanar)		TDDFT[b] (nonplanar)		DMRG[c]	SAC-CI (planar)	
PP*n*	ΔE (eV)	ΔE (eV)	f	ΔE (eV)	f	ΔE (eV)	ΔE (eV)	f
PP1	5.03	5.23	0.58	5.09	0.45	–	5.09	0.58
PP2	4.46	4.49	1.04	4.47	0.91	–	4.33	1.12
PP3	4.21	4.39	1.48	4.15	1.31	4.21	3.90	1.56
PP4	4.06	4.28	1.93	–	–	–	3.63	2.10

[a] From ref 58. Observed in cyclohexane/benezene. [b] From ref 20. [c] From ref 59.

TABLE 5: Vertical Excitation Energies (ΔE, eV) of Triplet Excited States of PP*n* with $n = 1-4$

PP*n*	SAC-CI (nonplanar)	DMRG[a]	SAC-CI (planar)
PP1	3.69	–	3.37
PP2	3.51	–	3.07
PP3	3.32	3.29	2.80
PP4	3.27	–	2.74

[a] From ref 59.

The lowest singlet vertical excitation energies for PP*n* are reported and compared with available experimental[58,59] and theoretical[20] values in Table 4, and the triplet transition energies are given in Table 5. Transition energies for both the nonplanar and planar cases are included in these tables. In the nonplanar case, the singlet excitation energies agree very well with the available experimental results; the mean deviation lies within 0.16 eV, and the maximum deviation is 0.22 eV. The experimental absorption spectra were observed in cyclohexane/benzene, for which the solvent effect is expected to be minor. The present results for the nonplanar case are compared with experimental[58] and TDDFT[20] values in Figure 4. The calculated transition energy decreases as the conjugation length increases, i.e., the transition becomes red-shifted with increasing chain length. The excitation energy is almost proportional to $1/(n + 1)$, as shown in Figure 4, although the deviation from linearity is large for PP2. The triplet state also shows a trend similar to that of the singlet state as the conjugation length increases. The singlet−triplet splitting decreases with increasing chain length, as shown in the Supporting Information. In all cases, we find that the triplet state is on the order of 0.9−1.7 eV below the singlet state, which indicates a localized triplet state with a large

TABLE 6: Lowest Singlet ($S_1 \rightarrow S_0$) Emission Energies (ΔE, eV) and Oscillator Strengths (f) of PP*n* Compared to Experimental Results

	expt[a]	SAC-CI (nonplanar)	
PP*n*	ΔE	ΔE	f
PP1	3.97	4.26	0.72
PP2	3.68	3.72	1.19
PP3	3.41	3.32	1.51
PP4	3.26	3.18	1.87

[a] From ref 58. Observed in cyclohexane/benezene.

exchange energy.[29] S_1 and T_1 both mainly correspond to single excitations from the HOMO to the LUMO. The SAC-CI emission energy from the S_1 state is summarized in Table 6 and compared with available experimental results.[58] It is evident from the table that the present emission spectra agree very well with the available experimental values; the mean deviation lies within 0.13 eV, and the largest deviation is 0.29 eV for PP1. The zero-point-energy correction to the S_0-S_1 transition energy was estimated as -0.16 eV for nonplanar PP1, where the ground and lowest excited states were calculated using the Hartree−Fock and CIS level of theories, respectively.

For the planar case, the excitation energies decrease more rapidly as the chain length increases, as seen in Tables 4 and 5. In the planar case, the π electrons are more delocalized over the oligomers than in the nonplanar case; as a consequence, the singlet and triplet states are more stabilized. These results might provide some insight for the development of new materials, as the molecules become more planar in longer polymers and in the crystalline state. In this case also, a large exchange energy, i.e., 0.89−1.72 eV, was obtained, and the singlet−triplet gap maintained a linear relationship.

Ground- and Excited-State Geometries

Poly(*para-phenylene vinylene) (PPVn, n = 1, ..., 4).* The ground-state and lowest singlet and triplet excited-state structures of PPV1 and PPV2 were optimized with the SAC-CI method restricted to a planar C_{2h} symmetry. The optimized ground-state geometry of PPV3 is given in the Supporting Information. For the S_0 state, we also performed a full optimization and confirmed that the stable geometry of the ground state of PPV*n* is planar. Optimization by the CIS method of the S_1 and T_1 states of PPV*n* considering a nonplanar initial geometry produced a planar structure. The ground- and excited-state geometries calculated by the SAC-CI method are summarized in Table 7 and compared with the experimental results.[60] The present ground-state geometry of PPV1 agrees very well with the experimental values;[60] deviations lie within 0.005 Å and 0.07° for the bond length and bond angle, respectively. The changes in bond length (Δr) along the CC conjugation due to singlet and triplet excitations in PPV1 and PPV2 are shown in Figure 5. In the lowest excited states, the central vinylene C═C bond length increases, whereas the vinylene C−C bond length decreases. These changes are localized within the central part of the oligomers. For example, the geometric changes in PPV2 due to excitation are significant on the central phenyl ring and neighboring vinylene units. Similar changes were also obtained for PPV3 and PPV4 (estimated by means of CIS method). In the case of PPV1, a significant change was found only for the central vinylene unit. For PPV1, the increase in the central vinylene C═C bond length is on the order of 0.05 Å and 0.10 Å for the singlet and triplet, respectively, and the decrease of the C−C vinyl bond length is on the order of 0.05 and 0.07 Å, respectively. The localization of the bond length changes within the central part of the molecule, indicating that the lowest singlet and triplet excitations of these molecules are also localized.

TABLE 7: Ground-State (S_0) and Lowest Singlet (S_1) and Triplet (T_1) Excited-State Geometries of PPV*n* Calculated by the SAC/SAC-CI Method[a]

	PPV1				PPV2		
	S_0						
parameter	SAC	expt[b]	S_1	T_1	S_0	S_1	T_1
R1	1.390	1.394	1.409	1.407	1.390	1.399	1.397
R2	1.391	1.393	1.376	1.376	1.391	1.386	1.387
R3	1.402	1.406	1.426	1.431	1.400	1.415	1.412
R4	1.477	1.472	1.422	1.410	1.474	1.441	1.447
R5	1.341	1.336	1.394	1.443	1.342	1.378	1.388
R6					1.472	1.425	1.414
R7					1.400	1.432	1.442
R8					1.387	1.370	1.362
R9					1.402	1.427	1.438
A1	127.1	126.4	126.3	125.8	126.8	126.5	126.5
A2	113.9	−	115.2	115.9	114.3	115.0	115.1

[a] Bond lengths and angles are in angstroms and degrees, respectively. Details of numbers for bonds and bond angles are given in Figure 5. [b] From ref 60.

The bond length alternation (BLA) along the CC conjugation length due to singlet and triplet excitations in PPV1 and PPV2 was also estimated. The BLA changes significantly in the excited states from that of the ground state. In the case of PPV1, the BLA decreases from ∼0.13 Å in S_0 to ∼0.03 Å in S_1. In T_1, the single- and double-bond character in the vinylene linkage is reversed. The BLA in the vinylene group is negative: approximately −0.03 Å. In both, the singlet and triplet states, the BLA in the phenyl rings is ∼0.04−0.06 Å, whereas in the ground state, it is ∼0.01 Å. In the case of PPV2, the BLA decreases from ∼0.13 Å in S_0 to ∼0.05 Å in S_1 and ∼0.06 Å in T_1. The central phenyl ring is also deformed in this case and adopts a semiquinoid character, with BLA values of ∼0.01, ∼0.06, and ∼0.08 Å in the S_0, S_1, and T_1, respectively. Larger bond length changes were obtained for the lowest triplet state than for the lowest singlet state. A similar trend in bond length changes due to triplet excitation was also obtained in the INDO/MRD-CI calculations.[13]

These changes in the geometry due to excitation can be explained using the ESF theory proposed by Nakatsuji.[43,44] We discuss here some of the geometric changes in the lowest excited states of PPV1 and PPV2 based on this theory. In ESF theory, the geometric relaxation in the excited state can be explained by the force acting on nuclei caused by changes in the electron distribution. The Coulombic force exerted on the nuclei induces movements of the nuclei to accompany the change in the electron distribution until the forces diminish at the excited-state geometry. Molecular shape in the ground and excited states is determined by the balancing of the atomic dipole (AD), exchange (EC), and gross charge (GC) forces. For details, readers can refer to the original articles.[43,44] The differences in SAC-CI electron density between the ground state and the lowest singlet/triplet excited state due to excitation in PPV1 are shown in Figure 6, and those for PPV2 are given in the Supporting Information. The differences in electron density between the singlet and triplet states are also shown in these figures. The electron density in the central vinylene C═C bond region decreases, and that in the vinylene C−C bond region increases. More precisely, the electron density in the σ-bond region increases, and that in the π-bond region decreases; this is a general trend in these PPV*n* molecules. The EC force along the central vinylene C═C bond decreases because of the decrement of electron density in the C═C bond region, whereas

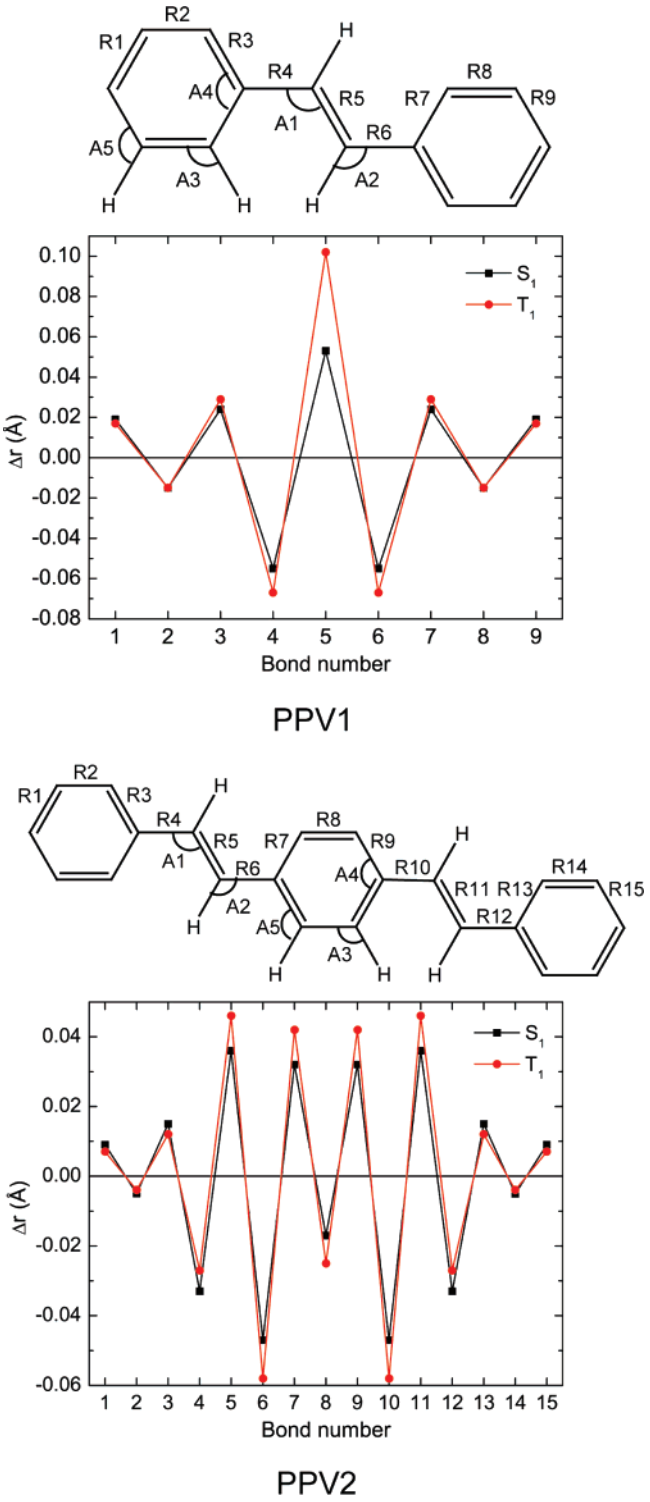

Figure 5. Changes in CC bond length (Δr) along the conjugation due to excitation in PPV1 and PPV2 calculated by the SAC-CI method.

the EC force is enhanced along the vinylene C—C bond. As a consequence, the central vinylene C═C bond length increases, and the vinylene C—C bond length decreases. The change in electron density due to excitation is more pronounced in the triplet state than in the singlet state, as is apparent from Figure 6 (S_1-T_1). This is the reason behind the larger change in bond length in the triplet state than in the singlet state.

In the case of singlet excitation, the electron distribution changes in the vicinity of some C nuclei, as is apparent from Figure 6 (S_0-S_1), whereas no such changes occur in the case of triplet transition. These accumulations (depletions) of electron

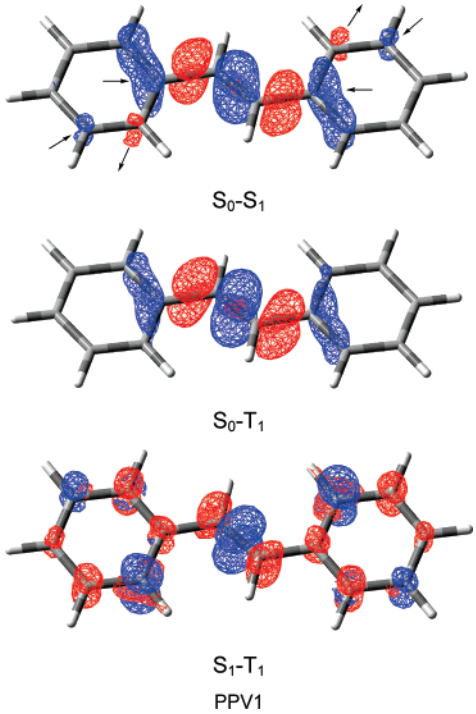

Figure 6. SAC-CI electron density differences between the ground state and the singlet/triplet excited states of PPV1 (interval = 0.003). S_1-T_1 corresponds to the electron density difference between the singlet and triplet states (interval = 0.001). The arrows denote the directions of force acting on the corresponding C nuclei. Blue, decrease; red, increase.

TABLE 8: Ground-State (S_0) and Lowest Singlet (S_1) and Triplet (T_1) Excited-State Geometries of PP*n* Calculated by the SAC/SAC-CI Method[a]

	PP1				PP2		
	S_0						
parameter	SAC	expt[b]	S_1	T_1	S_0	S_1	T_1
R1	1.393	1.395−1.425	1.413	1.419	1.393	1.403	1.401
R2	1.391	1.356−1.406	1.376	1.374	1.392	1.382	1.386
R3	1.403	−	1.439	1.440	1.402	1.423	1.419
R4	1.499	1.469−1.505	1.430	1.434	1.487	1.443	1.448
R5					1.400	1.432	1.444
R6					1.391	1.370	1.364
A1	119.6	115.0−118.3	119.5	119.2	119.3	119.2	119.2
A2	120.2	120.6−123.1	120.7	120.7	118.0	117.5	117.6
A3					117.2	117.0	116.8
θ	38.6	41.6,[c] 44.4[d]	36.3	36.5	37.9	36.7	36.9

[a] Bond lengths and angles are in angstroms and degrees, respectively. Details of numbers for bonds and bond angles are given in Figure 7. [b] From ref 62. [c] From ref 61. [d] From refs 63 and 64.

density are manifested by changes in the corresponding CCC/CCH angles. For example, in PPV1, angle A3 (details of numbers for bond angles are given in Figure 5) is enlarged in the singlet excited state (119.4°) from that in the ground state (118.3°) as a result of an accumulation of electron density in the region of the associated C nucleus. On the other hand, angle A5 is narrowed by 0.5°, from 120.1° to 119.6°, as a result of excitation as electron density depleted in the region of the associated C nucleus. From a similar argument, we can say that angle A4 decreases as a result of excitation. For this angle, the change is more pronounced in the triplet excited state (117.0°) than in the singlet excited state (117.3°); the ground-state value is 117.8°. In PPV2, angle A4 changes from 117.3° (ground state) to 116.7° (singlet excited state) and 116.4° (triplet excited state), and angle A3 changes from 118.6° (ground state) to 118.9° in

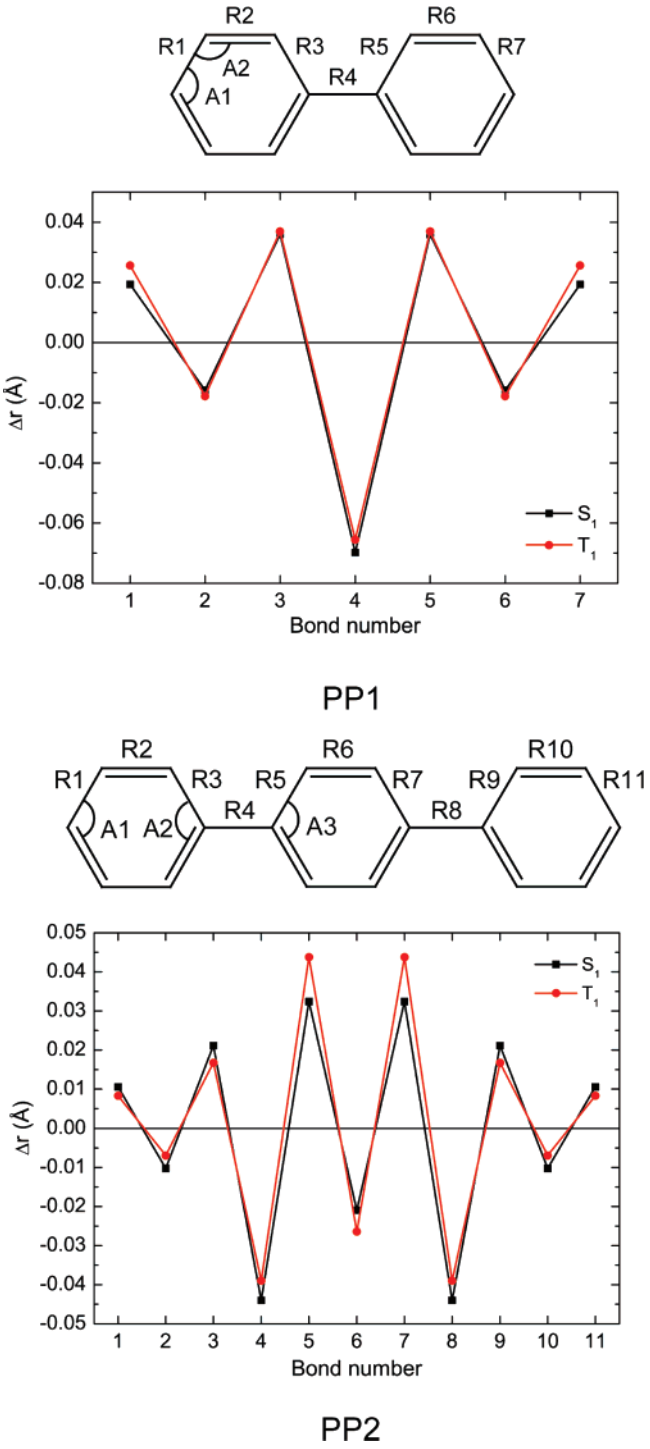

Figure 7. Changes in CC bond length (Δr) along the conjugation due to excitation in PP1 and PP2 calculated by the SAC-CI method.

the singlet excited state. The increase of angle A2 in the excited states is also due to the accumulation of electron density in the region of the C nuclei.

Poly(*para-phenylene) (PPn, n = 1, ..., 4).* The ground-state and lowest singlet and triplet excited-state structures of PP1 and PP2 were optimized with the SAC-CI method assuming a nonplanar D_2 symmetry. We performed full optimization for the ground state (S_0) and obtained stable geometries for PP*n*. The ground- and excited-state geometries calculated by the SAC-CI method are summarized in Table 8 and compared with the experimental results.[61−63] For the S_0, S_1, and T_1 states of PP1, we obtained torsion angles as 38.6°, 36.3°, and 36.5°, respectively. The corresponding values for PP2 are 37.9°, 36.7°, and

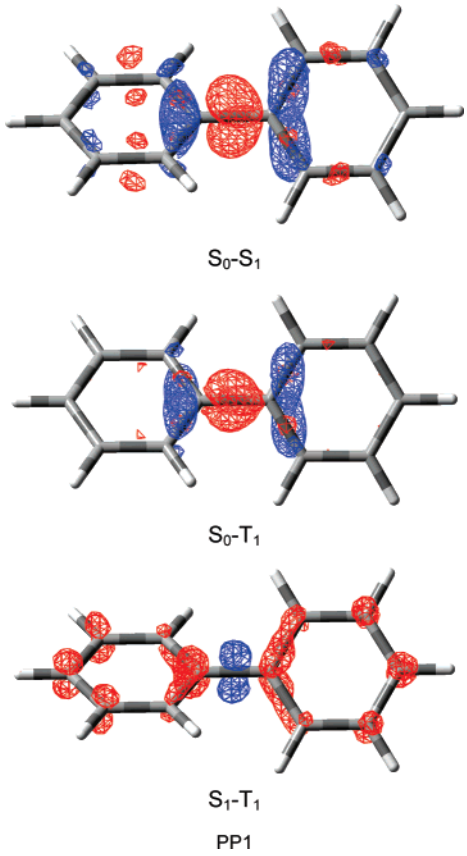

Figure 8. SAC-CI electron density differences between the ground state and the singlet/triplet excited states of PP1 (interval = 0.003). S_1-T_1 corresponds to the electron density difference between the singlet and triplet states (interval = 0.001). Blue, decrease; red, increase.

36.9°, respectively. Experimentally, the torsion angles obtained for the ground state of PP1 are 41.6°[61] and 44.4°,[63,64] which are in reasonable agreement with the present SAC-CI value of 38.6°.

The changes in bond length (Δr) along the CC conjugation due to singlet and triplet excitations in PP1 and PP2 are shown in Figure 7. In the lowest excited states, the C═C bond length increases, whereas the C—C bond length decreases. These changes are localized within the central part of the molecule, as in the case of PPV*n*. For example, the geometric changes in PP2 due to excitation are significant on the central phenyl ring. Similar changes were also obtained for PP3 and PP4 (estimated by means of CIS method). In PP1, the maximum increase of the C═C bond length is about 0.04 Å for both the singlet and triplet states, and the decrease in the C—C bond length is around 0.07 Å. In the case of PP2, the maximum increase of the C═C bond length is about 0.04 Å for both the singlet and triplet states, and the decrease in the C—C bond length is around 0.04 Å. The localization of the bond length changes within the central part of the molecule, indicating that the lowest singlet and triplet excitations of these molecules are also localized. In the excited state, the single bond joining the phenyl rings acquires a certain amount of double-bond character, and the inter-ring structure is forced into a more planar structure, as is clear from Table 8. This is also apparent from the values of the twisting angles for the ground and excited states.

The BLA changes significantly in the excited states from that of the ground state. For example, in PP1, the BLA decreases from ~0.1 Å in S_0 to ~0.06 Å in S_1 and T_1. In the case of PP2, the BLA decreases from ~0.09 Å in S_0 to ~0.06 Å in S_1 and ~0.08 Å in T_1. Larger bond length changes were obtained for

the lowest triplet state than for the lowest singlet state. From our SAC-CI calculations, we found that angles A1 and A2 do not change in the excited states. The differences in SAC-CI electron density between the ground and lowest singlet/triplet excited states due to excitation in PP1 are shown in Figure 8, and those in PP2 are given in the Supporting Information. The geometry relaxations in PP*n* can also be explained by ESF theory, as described in the previous subsection for PPV*n*.

Conclusions

Electronic spectra and ground- and low-lying excited-state geometries of oligomers of poly(*para*-phenylene vinylene) and poly(*para*-phenylene) were investigated using the SAC-CI method. The absorption and emission spectra were calculated very accurately, with the average deviation from the experimental results lying within 0.2 eV. The chain length dependence of the transition energies was reproduced correctly in the present computations. However, it is also true that SAC-CI calculations for larger oligomers, $n \geq 5$ in the present case, are very expensive. It turned out that conventional TDDFT with the B3LYP functional should be used carefully, because it can provide inaccurate estimates of the chain length dependence of $\pi\pi^*$ excitation energies for these molecules with long π-conjugated chains. It was found that, in all cases, the lowest triplet state is at a lower energy (1.0−1.5 eV for PPV*n* and 0.9−1.7 eV for PP*n*) than the lowest singlet state, which indicates a localized triplet state with a large exchange energy. For the oligomers studied in this research, there exists a linear relationship between singlet−triplet energy gap, and the triplet state is more localized than the singlet state. For *trans*-stilbene, the doubly excited 2^1A_g state was estimated at a value of 4.99 eV, which agrees very well with the experimental result of 4.84 eV. In contrast to previous ab initio calculations, we predict this 2^1A_g state to lie above the 1^1B_u state.

We discussed geometry relaxations in detail and explained them using electrostatic force theory. The maximum changes in bond length due to excitation in PPV*n* were obtained in the C═C and C−C vinylene bonds along the conjugation. The bond length changes were found to be mainly localized in the central part of the oligomers. Comparatively larger bond length changes were obtained for the triplet excited state than for the singlet excited state. This finding can also be explained in terms the calculated SAC-CI electron density difference between the singlet and triplet states. Comparisons with available experimental and other theoretical values showed that the SAC-CI method is useful for studying the electronic excitations and excited-state geometries of the oligomers of poly(*para*-phenylene vinylene) (PPV) and poly(*para*-phenylene) (PP).

The present results show that the SAC-CI method is useful for predicting the optical properties of OLED molecules with long π-conjugated chains and is suitable for the theoretical design of such OLED oligomers.

Acknowledgment. This study was supported by a Grant for Creative Scientific Research from the Ministry of Education, Science and Sports of Japan. B.S. is grateful to the Japan Society for the Promotion of Science (JSPS) for financial support.

Supporting Information Available: Comparison of the ground-state geometries optimized by SAC and DFT(B3LYP) with the 6-31G(d) basis set for PPV*n* ($n = 1-3$) and PP*n* ($n = 1, 2$) and excitation energies computed by SAC-CI/D95(d) at these geometries. Comparison of the S_1 state geometries of PPV1, PPV2, PP1, and PP2 optimized by SAC-CI and CIS with D95(d). Figures showing S_1-T_1 energy separations of PPV*n* and PP*n* and triplet excitation energies of PPV*n*. Comparison of the experimental absorption and emission spectra of PPV*n* ($n = 1-4$) with the SAC-CI spectra. Electron density difference structures for PPV2 and PP2. Optimized ground-state geometries of PPV3. This material is available free of charge via the Internet at http://pubs.acs.org.

References and Notes

(1) Burroughes, J. H.; Bradley, D. D. C.; Brown, A. R.; Marks, R. N.; McKay, K.; Friend, R. H.; Burn, P. L.; Holmes, A. B. *Nature (London)* **1990**, *347*, 539.
(2) Tessler, N.; Denton, G. J.; Friend, R. H. *Nature (London)* **1996**, *382*, 695.
(3) Friend, R. H.; Gymer, R. W.; Holmes, A. B.; Burroughes, J. H.; Marks, R. N.; Taliani, C.; Bradley, D. D. C.; Santos, D. A. D.; Brédas, J. L.; Logdlund, M.; Salaneck, W. R. *Nature (London)* **1999**, *397*, 121.
(4) Schenk, R.; Gregorius, H.; Müllen, K. *Adv. Mater.* **1991**, *3*, 492.
(5) Grem, G.; Leditzky, G.; Ullrich, B.; Leising, G. *Adv. Mater.* **1992**, *4*, 36.
(6) Barashkov, N. N.; Guerrero, D. J.; Olivos, H. J.; Ferraris, J. P. *Synth. Met.* **1995**, *75*, 153.
(7) Cornil, J.; Beljonne, D.; Heller, C. M.; Campbell, I.; Laurich, B. K.; Smith, D. L.; Bradley, D. D. C.; Mullen, K.; Brédas, J. L. *Chem. Phys. Lett.* **1997**, *278*, 139.
(8) Oelkrug, D.; Tompert, A.; Gierschner, J.; Egelhaaf, H.-J.; Hanack, M.; Hohloch, M.; Steinhuber, E. *J. Phys. Chem. B* **1998**, *102*, 1902.
(9) Mulazzi, E.; Ripamonti, A.; Wery, J.; Dulieu, B.; Lefrant, S. *Phys. Rev. B* **1999**, *60*, 16519.
(10) Nguyen, T. P.; Tran, V. H.; Destruel, P.; Oelkrug, D. *Synth. Met.* **1999**, *101*, 633.
(11) Ichino, Y.; Ni, J. P.; Ueda, Y.; Wang, D. K. *Synth. Met.* **2001**, *116*, 223.
(12) Gierschner, J.; Mack, H.-G.; Luer, L.; Oelkrug, D. *J. Chem. Phys.* **2002**, *116*, 8596.
(13) Beljonne, D.; Shuai, Z.; Friend, R. H.; Brédas, J. L. *J. Chem. Phys.* **1995**, *102*, 2042.
(14) Cornil, J.; dosSantos, D. A.; Crispin, X.; Silbey, R.; Brédas, J. L. *J. Am. Chem. Soc.* **1998**, *120*, 1289.
(15) Cornil, J.; Beljonne, D.; Brédas, J. L. *J. Chem. Phys.* **1995**, *103*, 834.
(16) Cornil, J.; Beljonne, D.; Shuai, Z.; Hagler, T. W.; Campbell, I.; Bradley, D. D. C.; Brédas, J. L.; Spangler, C. W.; Mullen, K. *Chem. Phys. Lett.* **1995**, *247*, 425.
(17) Zojer, E.; Cornil, J.; Leising, G.; Brédas, J. L. *Phys. Rev. B* **1999**, *59*, 7957.
(18) Tretiak, S.; Saxena, A.; Martin, R. L.; Bishop, A. R. *J. Phys. Chem. B* **2000**, *104*, 7029.
(19) Lavrentiev, M. Y.; Barfoed, W.; Martin, S. J.; Daly, H.; Bursill, R. J. *Phys. Rev. B* **1999**, *59*, 9987.
(20) Pogantsch, A.; Heimel, G.; Zojer, E. *J. Chem. Phys.* **2002**, *117*, 5921.
(21) Han, Y. K.; Lee, S. U. *J. Chem. Phys.* **2004**, *121*, 609.
(22) Shukla, A. *Phys. Rev. B* **2002**, *65*, 125204.
(23) Shukla, A.; Ghosh, H.; Mazumdar, S. *Phys. Rev. B* **2003**, *67*, 245203.
(24) Brown, A. R.; Pichler, K.; Greenham, N. C.; Bradley, D. D. C.; Friend, R. H. *Chem. Phys. Lett.* **1993**, *210*, 61.
(25) Karabunarliev, S.; Baumgarten, M.; Müllen, K. *J. Phys. Chem. A* **2000**, *104*, 8236.
(26) Brédas, J. L.; Thémans, B.; André, J. M. *Phys. Rev. B* **1982**, *26*, 6000.
(27) Brédas, J. L.; Thémans, B.; Fripiat, J. G.; André, J. M.; Chancé, R. R. *Phys. Rev. B* **1984**, *29*, 6761.
(28) Soos, Z. G.; Etemad, S.; Galvão, D. S.; Ramasesha, S. *Chem. Phys. Lett.* **1992**, *194*, 341.
(29) Köhler, A.; Beljonne, D. *Adv. Funct. Mater.* **2004**, *14*, 11.
(30) Tian, B.; Zerbi, G.; Schenk, R.; Müllen, K. *J. Chem. Phys.* **1991**, *95*, 3191.
(31) Tian, B.; Zerbi, G.; Müllen, K. *J. Chem. Phys.* **1991**, *95*, 3198.
(32) Molina, V.; Merchan, M.; Roos, B. O. *J. Phys. Chem. A* **1997**, *101*, 3478.
(33) Kwasniewski, S. P.; Deleuze, M. S.; Francois, J. P. *Int. J. Quantum Chem.* **2000**, *80*, 672.
(34) Beljonne, D.; Cornil, J.; Brédas, J. L.; Friend, R. H. *Synth. Met.* **1996**, *76*, 61.
(35) Ambrosch-Draxl, C.; Majewski, J. A.; Vogl, P.; Leising, G. *Phys. Rev. B* **1995**, *51*, 9668.
(36) Capaz, R. B.; Caldas, M. J. *J. Mol. Struct. (THEOCHEM)* **1999**, *464*, 31.

(37) Capaz, R. B.; Caldas, M. J. *Phys. Rev. B* **2003**, *67*, 205205.
(38) Alves-Santos, M.; Davila, L. Y. A.; Petrilli, H. M.; Capaz, R. B.; Caldas, M. J. *J. Comput. Chem.* **2006**, *27*, 217.
(39) Nakatsuji, H. *Chem. Phys. Lett.* **1978**, *59*, 362.
(40) Nakatsuji, H.; Hirao, K. *J. Chem. Phys.* **1978**, *68*, 2053.
(41) Nakatsuji, H. *Chem. Phys. Lett.* **1979**, *67*, 334; *Chem. Phys. Lett.* **1979**, *67*, 329.
(42) Nakatsuji, H.; Miyahara, T.; Fukuda, R. *J. Chem. Phys.* **2007**, *126*, 084104.
(43) Nakatsuji, H. *J. Am. Chem. Soc.* **1973**, *95*, 345.
(44) Nakatsuji, H.; Koga, T. In *The Force Concept in Chemistry*; Deb, B. M., Ed.; Van Nostrand Reinhold Company: New York, 1981; p 137.
(45) Dunning, T. H., Jr.; Hay, P. J. In *Modern Theoretical Chemistry*; Schaefer, H. F., III, Ed.; Plenum Press: New York, 1976; Vol. 3.
(46) Nakatsuji, H. *Chem. Phys. Lett.* **1991**, *177*, 331. Nakatsuji, H. In *Computational Chemistry—Review of Current Trends*; Leszczynski, J., Ed.; World Scientific: Singapore, 1997; Vol. 2, p 62.
(47) Ishida, M.; Toyota, K.; Ehara, M.; Nakatsuji, H. *Chem. Phys. Lett.* **2001**, *347*, 493.
(48) Nakatsuji, H. *Chem. Phys.* **1983**, *75*, 425.
(49) Frisch, M. J.; Trucks, G. W.; Schlegel, H. B.; Scuseria, G. E.; Robb, M. A.; Cheeseman, J. R.; Montgomery, J. A., Jr.; Vreven, T.; Kudin, K. N.; Burant, J. C.; Millam, J. M.; Iyengar, S. S.; Tomasi, J.; Barone, V.; Mennucci, B.; Cossi, M.; Scalmani, G.; Rega, N.; Petersson, G. A.; Nakatsuji, H.; Hada, M.; Ehara, M.; Toyota, K.; Fukuda, R.; Hasegawa, J.; Ishida, M.; Nakajima, T.; Honda, Y.; Kitao, O.; Nakai, H.; Klene, M.; Li, X.; Knox, J. E.; Hratchian, H. P.; Cross, J. B.; Bakken, V.; Adamo, C.; Jaramillo, J.; Gomperts, R.; Stratmann, R. E.; Yazyev, O.; Austin, A. J.; Cammi, R.; Pomelli, C.; Ochterski, J. W.; Ayala, P. Y.; Morokuma, K.; Voth, G. A.; Salvador, P.; Dannenberg, J. J.; Zakrzewski, V. G.; Dapprich, S.; Daniels, A. D.; Strain, M. C.; Farkas, O.; Malick, D. K.; Rabuck, A. D.; Raghavachari, K.; Foresman, J. B.; Ortiz, J. V.; Cui, Q.; Baboul, A. G.; Clifford, S.; Cioslowski, J.; Stefanov, B. B.; Liu, G.; Liashenko, A.; Piskorz, P.; Komaromi, I.; Martin, R. L.; Fox, D. J.; Keith, T.; Al-Laham, M. A.; Peng, C. Y.; Nanayakkara, A.; Challacombe, M.; Gill, P. M. W.; Johnson, B.; Chen, W.; Wong, M. W.; Gonzalez, C.; Pople, J. A. *Gaussian 03*; revision C02; Gaussian, Inc.: Pittsburgh, PA, 2003.
(50) Miertus S.; Scrocco V.; Tomasi J. *Chem. Phys.* **1981**, *55*, 117.
(51) Albota, M.; Beljonne, D.; Brédas, J.-L.; Ehrlich, J. E.; Fu, J.-Y.; Heikal, A. A.; Hess, S. E.; Kogej, T.; Levin, M. D.; Marder, S. R.; McCord-Maughon, D.; Perry, J. W.; Rockel, H.; Rumi, M.; Subramaniam, G.; Webb, W. W.; Wu, X.-L.; Xu, C. *Science* **1998**, *281*, 1653.
(52) Shuai, Z.; Brédas, J. L. *Phys. Rev. B* **2000**, *62*, 15452.
(53) Soos, Z. G.; Ramasesha, S.; Galvao, D. S.; Etemad, S. *Phys. Rev. B* **1993**, *47*, 1742.
(54) Saha, B.; Ehara, M.; Nakatsuji, H. *J. Chem. Phys.* **2006**, *125*, 014316.
(55) Monkman, A. P.; Burrows, H. D.; Hartwell, L. J.; Horsburgh, L. E.; Hamblett, I.; Navaratnam, S. *Phys. Rev. Lett.* **2001**, *86*, 1358.
(56) Briks, J. B. *Photophysics of Aromatic Molecules*; John Wiley & Sons: London, 1970.
(57) Beljonne, D.; Cornil, J.; Friend, R. H.; Janssen, R. A. J.; Brédas, J. L. *J Am. Chem. Soc.* **1996**, *118*, 6453.
(58) Nijegrodov, N. I.; Downey, W. S.; Danailov, M. B. *Spectrochim. Acta A* **2000**, *56*, 783.
(59) Moore, E. E.; Barford, W.; Bursill, R. J. *Phys. Rev. B* **2005**, *71*, 115107.
(60) Hoekstra, A.; Meertens, P.; Vos, A. *Acta Crystallogr. B* **1975**, *31*, 2813.
(61) Almenningen, A.; Bastiansen, O. *K. Nor. Vidensk. Selsk. Skr.* **1958**, (No. 4), 1.
(62) Baudour, J. L.; Cailleau, H.; Yelon, W. B. *Acta Crystallogr. B: Struct. Crystallogr. Cryst. Chem.* **1977**, *33*, 1713.
(63) Almenningen, A.; Bastiansen, O.; Fernholt, L.; Cyvin, B. N.; Cyvin, S. J.; Samdal, S. *J. Mol. Struct.* **1985**, *128*, 59.
(64) Bastiansen, O.; Samdal, S. *J. Mol. Struct.* **1985**, *128*, 115.